Available online at www.sciencedirect.com
SCIENCE DIRECT
Journal of Magnetic Resonance 178 (2006) 206–211
JMR Journal of Magnetic Resonance
www.elsevier.com/locate/jmr

Cooling overall spin temperature: Protein NMR experiments optimized for longitudinal relaxation effects

Michaël Deschamps [a,b,*], Iain D. Campbell [b]

[a] CRMHT-CNRS, 1D Avenue de la Recherche Scientifique, 45071 Orléans Cedex 2, France
[b] Department of Biochemistry, University of Oxford, South Parks Road, OX1 3QU Oxford, UK

Received 22 July 2005; revised 9 September 2005
Available online 24 October 2005

Abstract

In experiments performed on protonated proteins at high fields, 80% of the NMR spectrometer time is spent waiting for the ^{1}H atoms to recover their polarization after recording the free induction decay. Selective excitation of a fraction of the protons in a large molecule has previously been shown to lead to faster longitudinal relaxation for the selected protons [K. Pervushin, B. Vögeli, A. Eletsky, Longitudinal ^{1}H relaxation optimization in TROSY NMR spectroscopy, J. Am. Chem. Soc. 124 (2002) 12898–12902; P. Schanda, B. Brutscher, Very fast two-dimensional NMR spectroscopy for real-time investigation of dynamic events in proteins on the time scale of seconds, J. Am. Chem. Soc. 127 (2005) 8014–8015; H.S. Attreya, T. Szyperski, G-matrix Fourier transform NMR spectroscopy for complete protein resonance assignment, Proc. Natl. Acad. Sci. USA 101 (2004) 9642–9647]. The pool of non-selected protons acts as a ''thermal bath'' and spin-diffusion processes (''flip-flop'' transitions) channel the excess energy from the excited pool to the non-selected protons in regions of the molecule where other relaxation processes can dissipate the excess energy. We present here a sensitivity enhanced HSQC sequence (COST-HSQC), based on one selective E-BURP pulse, which can be used on protonated ^{15}N enriched proteins (with or without ^{13}C isotopic enrichment). This experiment is compared to a gradient sensitivity enhanced HSQC with a water flip-back pulse (the water flip-back pulse quenches the spin diffusion between $^1H^N$ and $^1H^\alpha$ spins). This experiment is shown to have significant advantages in some circumstances. Some observed limitations, namely sample overheating with short recovery delays and complex longitudinal relaxation behaviour are discussed and analysed.

Keywords: Polarization recovery delay; Longitudinal relaxation; HSQC; Relaxation-optimized spectroscopy; Signal-to-noise ratio

1. Introduction

Most experiments include a delay d_1 for the recovery of longitudinal magnetization after recording the free induction decay (FID). The recovery delay d_1 is usually set to 1–5 times the longitudinal relaxation time-constant (T_1) where T_1 for deuterated proteins can be as long as 10 s. With mono-exponential relaxation, characterized by a single time constant T_1, the optimal interscan delay d_1 is equal to $1.25 \times T_1 - d_0$, where d_0 is the pulse sequence duration [1–3]. A significant fraction of the NMR spectrometer time is thus spent waiting for system recovery. For proteins, the T_1 value and linewidth ($\sim 1/T_2$) usually increase with the correlation time τ_c (>1 ns) thus giving a size limit to protein studies. Substituting most of the ^{1}H atoms with ^{2}H atoms leads to a line sharpening of the amide protons and facilitates the use of TROSY experiments [4] but ^{2}H isotopic enrichment further increases T_1.

In large protonated proteins, the ^{1}H longitudinal relaxation rates are usually dominated by spin diffusion and the relaxation rate of rotating methyl groups [5]. A more detailed study of the relaxation properties of a two-spin system is given in Appendix A [6]. Radiofrequency pulses perturb the spin system and, usually, a portion of the spin system has no net polarization after the acquisition period. For small molecules, the double-quantum W_2 and single-quantum W_1 transition probabilities (proportional to the

* Corresponding author.
E-mail address: michael.deschamps@cnrs-orleans.fr (M. Deschamps).

1090-7807/$ - see front matter © 2005 Elsevier Inc. All rights reserved.
doi:10.1016/j.jmr.2005.09.011

spectral density functions $J(2\omega_0)$ and $J(\omega_0)$, respectively) are high and such transitions dissipate the energy of the system. For large molecules, W_0 (proportional to $J(0)$), or "flip-flop" transition probabilities dominate and these do not dissipate energy but they channel it to other regions of the system where other relaxation mechanisms occur.

Hence, for a protein HSQC spectrum, where only amide protons ($^1H^N$) are observed, the input of energy should be minimized, and the resonances of protons other than amides should not be perturbed. Thus, the $-R_{\text{cross}}(\langle I_{Bz}\rangle - \langle I_{Bz}^{\text{eq}}\rangle)$ term stemming from these protons is initially zero instead of being negative, resulting in faster longitudinal relaxation and a shorter effective recovery time as shown in Appendix A.

2. Results and discussion

2.1. Longitudinal relaxation behaviour

The effectiveness of quenching the cross-relaxation contributions can be studied via band-selective and non-selective inversion-recovery experiments, which characterize longitudinal relaxation. In our case, these experiments were followed by a ^1H, ^{15}N HSQC filter, using a 3 s recovery delay between scans. Two experiments were performed on a ^{15}N, ^{13}C enriched pair of human fibronectin modules, $^4F1^5F1$ [7]: first, a non-selective inversion-recovery experiment, with a short non-selective 180° pulse, and second, a selective inversion recovery with an I-BURP pulse [8], which inverts the amide protons selectively, as described in Section 4. Almost no saturation was observed when using the I-BURP pulse, with signal intensities in the inverted region for the selective case being $\geqslant 90\%$ of the intensities of the non-selective experiment. The longitudinal relaxation behaviour of $H^N{}_{73}$, when all protons (non-selective case) or when the amide protons (selective case) are inverted, is shown in Fig. 1 as an example of what is observed for most of the amide protons.

Quenching the cross-relaxation term works very well initially, and initial R_1 rates are ten times larger in the selective case than in the non-selective case (Fig. 2). However, the inversion of amide protons perturbs the neighbouring protons, and their polarization states are modified (i.e., through a NOE transfer). Hence, the cross-relaxation term reappears, and the relaxation is slowed down, which explains why a second regime appears, with longer longitudinal relaxation time-constants T_{1l} (compare [1]). For selective inversion of residue 73, the recovery can be analysed in terms of two exponentials with one short, $T_{1s} = 54.1 \pm 1.8$ ms, and one long, $T_{1l} = 388.3 \pm 33.1$ ms, time-constant. A simple example is treated analytically in Appendix A to give a better understanding of the situation. The characterization of the second time-constant is sometimes difficult, especially for residues where the T_{1l} value is larger than the maximum delay (1.5 s), leading to large errors in the fitted T_{1l}. For non-selective inversion, one single time-constant $T_1 = 962.1 \pm 88.6$ ms is sufficient to fit

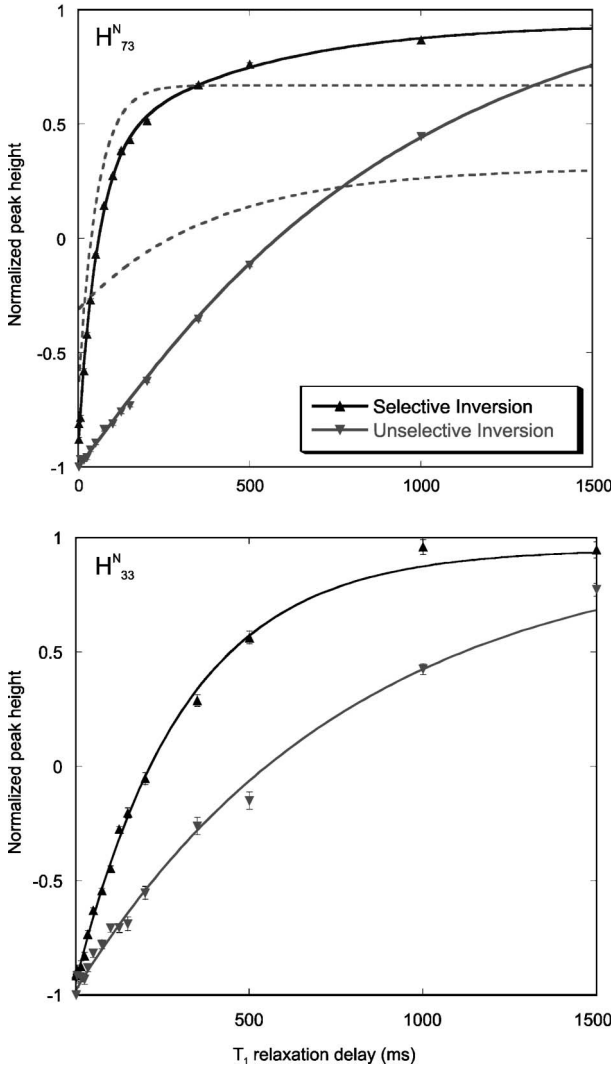

Fig. 1. Longitudinal relaxation behaviour for the amide proton of residue 73 and 33 in $^4F1^5F1$, for non-selective (grey ∇) and band selective (black ▲—all amide protons together) inversion recovery experiments (180°–T_1 relaxation delay–HSQC–recovery delay). $H^N{}_{73}$: Like most amide protons, the relaxation in the non-selective case can be described by a mono-exponential curve and a single T_1 constant ($T_1 = 962.1 \pm 88.6$ ms), whereas the relaxation in the selective case can only be described by a bi-exponential function, with one short ($T_{1s} = 54.1 \pm 1.8$ ms) and one long ($T_{1l} = 388.3 \pm 33.1$ ms) time constants. The fast and slow component have been separated, with respective weight 0.68 and 0.32, and plotted on the graph (dashed lines). $H^N{}_{33}$: In both cases, the relaxation is described by a single exponential with a selective $T_1 = 310.4 \pm 7.0$ ms and an unselective $T_1 = 793.9 \pm 25.0$ ms.

the relaxation behaviour of $^1H^N{}_{73}$. For residue 33, the longitudinal relaxation behaviour is somewhat different: both selective and unselective inversions give rise to apparent monoexponential relaxation, with T_1 time constants of 310.4 ± 7.0 and 793.9 ± 25.0 ms, respectively.

For non-selective inversion, the range of initial T_1 values is between 700 ms and 2 s, with a median of 1.27 s, and a standard deviation of 380 ms. For selective inversion, the range is smaller, between 47.5 and 426.6 ms, with a median of 93.9 ms and a standard deviation of 50.5 ms. Only nine residues have initial T_1 constants longer than 150 ms

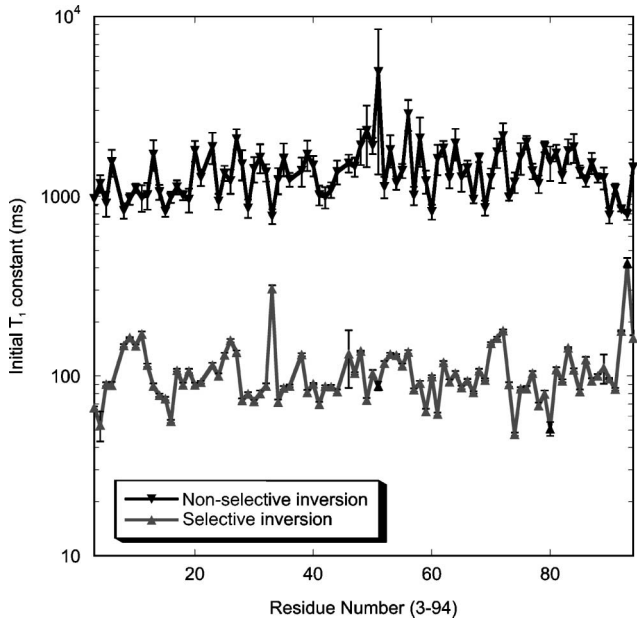

Fig. 2. Comparison between initial T_1 time-constants in the selective and non-selective inversion recovery experiment, observed for recovery delays ranging between 1 and 125 ms.

(residues 70, 26, 71, 9, 11, 92, 72, 33, 93 fall in the range from 150 to 426.6 ms). Residues 33 and 93 seem to have mono-exponential relaxation behaviour in both selective and unselective cases. Half of the residues have initial T_1 constants between 82 and 115 ms. Fig. 3 highlights these initial T_1 constants, measured for each amide proton in the protein. 25% of the residues (23 a.a., highlighted in red) of ^{4}F1^{5}F1 have initial T_1 constants less than 82 ms. A detailed study of possible relaxation effects, including cross-correlation between CSA/dipolar interaction and long-lived H^N-HOH dipolar interactions, has been published for another protein [10]. The most likely explanation for the unusually slow relaxation (blue residues in Fig. 3) is either local backbone mobility or cross-relaxation with neighbouring amide protons. These results emphasize that in COST-NMR experiments, where only amide protons are excited, recovery delays, $d_1 \geqslant 400$ ms are sufficient to allow the slowly relaxing protons to recover. Using too short recovery delays might lead to the saturation of these protons.

2.2. The COST-HSQC experiment

We have designed a new experiment, called COST-HSQC to utilize selective amide inversion or "cooling overall spin temperature (COST)." It is based on a gradient sensitivity enhanced HSQC [11] (Fig. 4A) and uses a band-selective E-BURP pulse on the amide protons (Fig. 4B). This experiment can be independently used on both ^{15}N and ^{15}N, ^{13}C enriched and protonated proteins. The previously published TROSY sequences optimized for longitudinal relaxation [1] require either 100% ^{13}C isotopic enrichment or several selective pulses. The SOFAST-HMQC [2] experiment also requires two selective pulses and uses Ernst-angle excitation. It is specifically designed for very short interscan delays. A very thorough comparison between HSQC and HMQC experiments in proteins has already been published [12]. In the COST-HSQC experiment, the use of an E-BURP pulse on H^N protons with a 0° phase, followed by a 90° pulse with a 270° ($-y$) phase, allows the creation of $H^N{}_zN_z$ after the fourth proton pulse and leaves the magnetization of all the other protons (including water) near the equilibrium state (H_z). Only the resonances located within the excitation bandwidth of the E-BURP pulse are observed, which might lead to the loss of high field H^N signals, which are located near the water frequency. Excitation of these resonances near the water peak might lead to degradation of the water flip back. The magnetization of the other protons spends some time in the xy plane and undergoes transverse relaxation. Hence, the flipped-back magnetization might not be exactly at its equilibrium value just before acquisition. A purge gradient is used before the first 90° pulse on nitrogen spins. Afterwards, the sequences are the same.

Another element must also be considered: the water flip-back pulse (E-SNOB [13]) will flip back the magnetization of some of the H^α protons which are usually located between 4.0 and 4.75 ppm [14]. Hence, the HSQC experiment which includes a water flip-back pulse is already 'longitudinal-relaxation optimized,' because the neighbouring H^α protons are kept in the equilibrium state. However, we show here that a median 20% signal improvement can be obtained using the COST-HSQC when a recovery delay

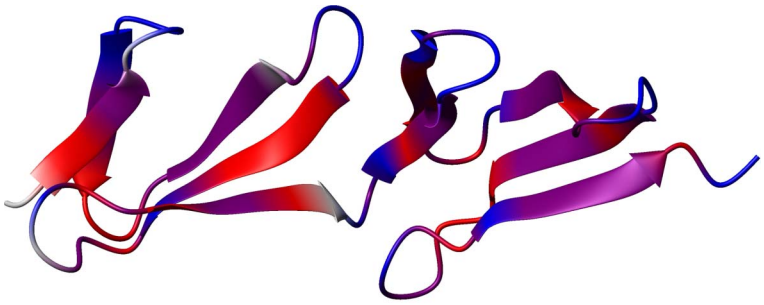

Fig. 3. Structure of the pair of fibronectin module ^{4}F1^{5}F1 (1FBR.pdb). Residues whose amide protons have an initial T_1 time constant shorter than 82 ms (first quartile) are shown in red; residues with initial T_1 constants longer than 115 ms (last quartile) are shown in blue and the remaining 50%, with initial T_1 constants between 82 and 115 ms, are shown in purple. The residues for which no result was available (residues 2, 7, 22, 37, and 45) are shown in white. The figure was made with MolMol [9].

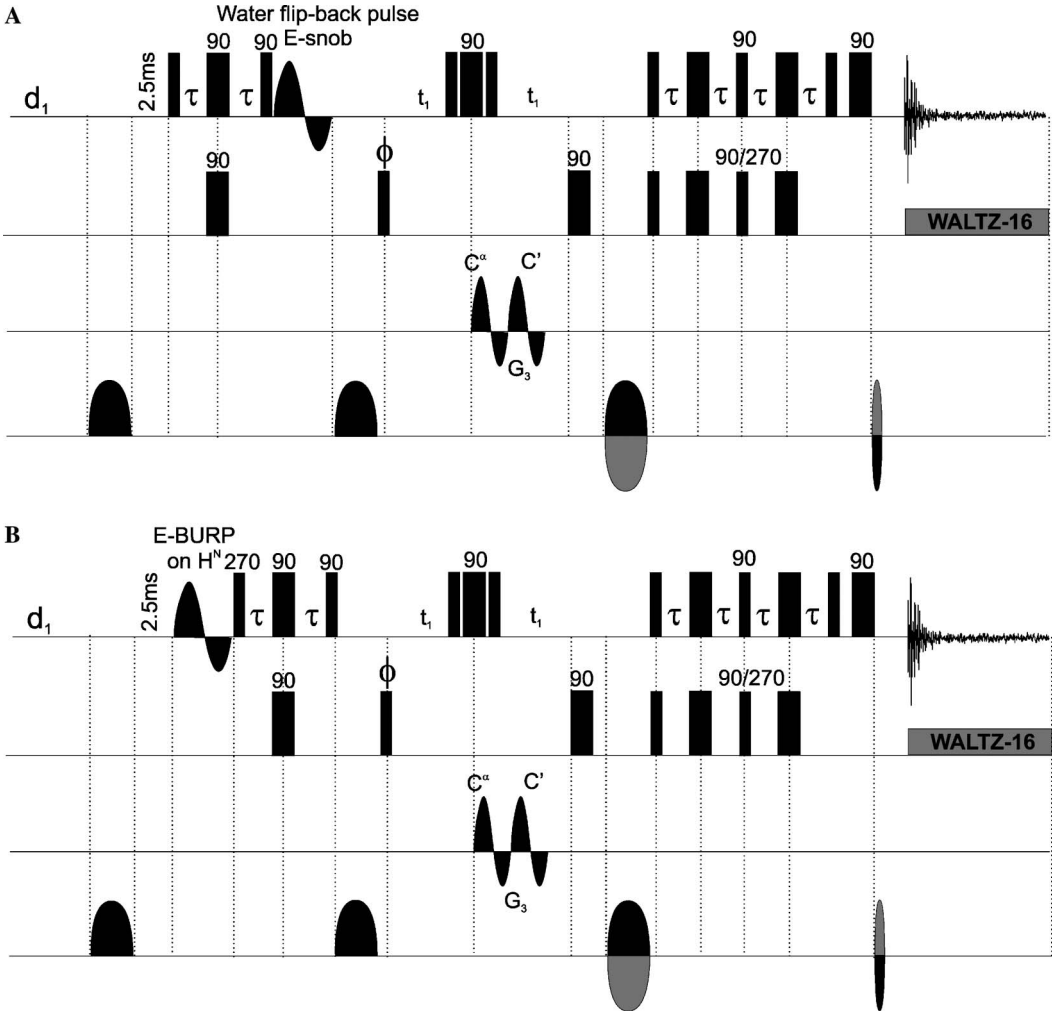

Fig. 4. Schemes for (A) the reference [11] and (B) COST (cooling overall spin temperature) HSQC experiments. When different from 0, pulse phases are indicated on the top of the squares representing the radiofrequency pulses.

$d_1 = 1$ s is used. The peak heights of each ^{15}N $^{1}H^{N}$ pair from $^{4}F1^{5}F1$ have been compared in the two experiments, i.e., the standard and the COST-HSQCs. The ratios between the standard and the COST peak heights are shown for every residues in Fig. 5, for six different d_1 delays (500, 750 ms, 1, 1.5, 2, and 3 s). The median signal improvements were calculated and were found to be 1.25, 1.20, 1.20, 1.18, 1.10, and 1.08 for d_1 delays of 500, 750 ms, 1, 1.5, 2, and 3 s, respectively. The dispersion between improvement values is quite high, ratios between 1.1 and 1.9 are observed for $d_1 = 500$ ms, and this can be explained by the different longitudinal relaxation behaviour of residues.

For $d_1 = 1$ s, the COST-HSQC gives a median gain of 20%, and the signal to noise ratio which is observed for a standard HSQC with $d_1 = 3$ s is recovered in 1 s using the COST-HSQC. A recovery delay of 1 s is commonly used for proteins, even if the complete recovery of polarization takes longer. Hence, the optimization of NMR experiments to create conditions for a faster polarization recovery can easily increase the measured peak intensities in protonated biomolecules.

There are, however, a few limitations: for some residues the selective T_1 is still around several hundreds of milliseconds; in addition, the use of very short recovery delays (250 ms) led to small observed chemical shift changes (≈0.01 ppm), attributed to a small rise of the sample temperature (≈1 °C) [15,16], which are certainly due to the use of ^{15}N decoupling during the acquisition time (81 ms) and the presence of buffer salts (≈50–100 mM). This effect can usually be reduced by using shorter acquisition time (if compatible with T_2 values of the fast relaxing residues), or L-TROSY experiments (which do not make use of ^{15}N decoupling) or by reducing the concentration of charged species in solution.

3. Conclusions

We have presented a new HSQC experiment which is optimized to speed up the recovery of polarization during the inter-scan delay by partial recovery (or flip-back) of unused proton polarization to cool the overall spin temperature. This is achieved by leaving the unobserved protons in the equilibrium position. The COST-HSQC uses

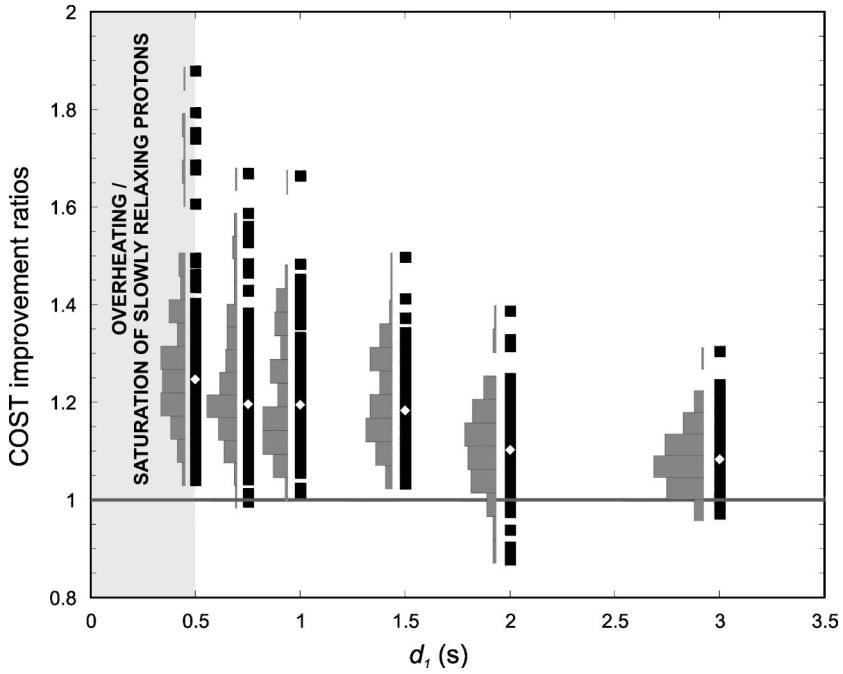

Fig. 5. COST improvement ratios (■) for each peak as a function of d_1, with the median value (♦) calculated over all the residues. The distribution of the ratio values is plotted vertically (grey squares). Below 500 ms, the water and protein chemical shifts are changing slightly (~0.01 ppm), indicating some heating of the sample (~1 °C) due to the short duty cycle and the salt content of the sample (~50–100 mM).

a single E-BURP pulse, band-selective for the amide proton region, in a modified gradient sensitivity enhanced HSQC experiment. The longitudinal relaxation behaviour of amide protons in a protein were analysed to determine the limits of COST.

COST can be used for d_1 longer than 500 ms, to avoid saturation of $^1H^N$ protons with slow selective longitudinal relaxation and to prevent mild sample heating in some unfavourable cases, leading to an average gain of 20% in peak heights for $d_1 = 1$ s for a 93 residues protein at 750 MHz and a temperature of 8 °C. Larger gains (up to 90%) have been observed for individual residues.

4. Experimental

The ^{4}F1^{5}F1 protein (93 residues) was expressed as described elsewhere [7] and all NMR measurements were performed at temperature $T = 8$ °C on a spectrometer operating at 750 MHz for ^{1}H and the pH of the samples was adjusted to 5.0. The selective pulses for inversion and excitation were I-BURP2 and E-BURP2 pulses, respectively [8], with pulse length of 1221 and 1333 μs (bandwidth ≈3700 Hz or 4.93 ppm, centered at 8.17 ppm) and maximum amplitudes 1.72 and 3.08 kHz, respectively. For inversion-recovery experiments, a 1 ms purge gradient was used, followed by fifteen different recovery delays: 1, 5, 15, 25, 35, 50, 75, 100, 125, 150, 200, 350, 500, 1000, and 1500 ms (Fig. 2). Longitudinal relaxation fitted well with a single exponential function in the non-selective case, and no improvement was detected using a bi-exponential function, as checked with an F test. In the selective case, a bi-exponential function was necessary to fit the data correctly. Initial T_1 time constants were calculated by fitting the peak intensities with a single exponential on the first nine delays (1–125 ms, see Fig. 3). The water flip-back pulse was a time reversed E-SNOB pulse [13] with pulse length equal to 2 ms and maximum amplitude of 8.35 kHz (bandwidth = 700 Hz or 0.93 ppm, centered on water). An acquisition time of 81 ms was used with a data size of 1024 complex points. Delay τ was set to 2.75 ms ($1/4J_{NH}$).

Acknowledgments

This work was supported by an EMBO fellowship and by the European Union through the research Training Network 'Cross-Correlation' for MD. IDC acknowledges support from the Welcome Trust.

Appendix A

The longitudinal relaxation of a proton spin can be described by the Solomon equations

$$\frac{d\langle I_{Az}\rangle}{dt} = -R_{auto}(\langle I_{Az}\rangle - I_{Az}^{eq}) + R_{cross}(\langle I_{Bz}\rangle - I_{Bz}^{eq}) \quad \text{with}$$

$$R_{auto} = W_0 + 2W_1 + W_2 \text{ and } R_{cross} = W_0 - W_2,$$

$$\frac{d\langle I_{Bz}\rangle}{dt} = R_{cross}(\langle I_{Az}\rangle - I_{Az}^{eq}) - R_{auto}(\langle I_{Bz}\rangle - I_{Bz}^{eq}) \quad \text{and}$$

$$\langle I_{Az}\rangle - I_{Az}^{eq} \leqslant 0;\ \langle I_{Bz}\rangle - I_{Bz}^{eq} \leqslant 0. \qquad (1)$$

The R_{auto} term contributes to the relaxation towards equilibrium, while the dipolar R_{cross} term can either make relaxation faster (R_{cross} is negative when $W_2 > W_0$ for small molecules, i.e., τ_c is short) or slower (R_{cross} is positive when

$W_2 < W_0$ for larger molecules when τ_c is long in the "spin diffusion limit").

For a system with N spins, the relaxation properties have to be studied using the whole relaxation matrix with N different eigenvalues and eigenvectors. Such a task depends upon the system geometry and many other parameters which are beyond the scope of this paper. If one looks at a two spin system, however, one can already have a simplified idea about relaxation behaviours in the selective and non-selective cases. The relaxation properties can be described by:

$$\begin{aligned}\frac{d\langle I_{Az}\rangle}{dt} &= -R^A_{\text{auto}}(\langle I_{Az}\rangle - I^{\text{eq}}_{Az}) + R_{\text{cross}}(\langle I_{Bz}\rangle - I^{\text{eq}}_{Bz})\\ \frac{d\langle I_{Bz}\rangle}{dt} &= R_{\text{cross}}(\langle I_{Az}\rangle - I^{\text{eq}}_{Az}) - R^B_{\text{auto}}(\langle I_{Bz}\rangle - I^{\text{eq}}_{Bz}),\end{aligned} \tag{2}$$

where R^X_{auto} is a phenomenological constant describing the global longitudinal relaxation properties of spin X, and R_{cross} describes the cross-relaxation term. In the selective inversion case, $\langle I_{Az}\rangle = -I^{\text{eq}}_{Az}$ and $\langle I_{Bz}\rangle = I^{\text{eq}}_{Bz}$ initially, whereas in the non-selective inversion case, the initial conditions are $\langle I_{Az}\rangle = -I^{\text{eq}}_{Az}$ and $\langle I_{Bz}\rangle = -I^{\text{eq}}_{Bz}$.

This problem can be solved analytically, using $R = (R^A_{\text{auto}} + R^B_{\text{auto}})/2$ and $d = (R^A_{\text{auto}} - R^B_{\text{auto}})/2$; or $R^A_{\text{auto}} = R + d$ and $R^B_{\text{auto}} = R - d$, where $-R \leqslant d \leqslant R$. Two eigenvalues are obtained, i.e., a slow component $(R - \sqrt{d^2 + R^2_{\text{cross}}})$ and a fast component $(R + \sqrt{d^2 + R^2_{\text{cross}}})$.

In the non-selective case

$$\begin{aligned}\langle I_{Az}\rangle = I^{\text{eq}}_{Az}\Bigg(1 - \left[1 + \frac{d + R_{\text{cross}}}{\sqrt{d^2 + R^2_{\text{cross}}}}\right] e^{-\left(R - \sqrt{d^2 + R^2_{\text{cross}}}\right)t}\\ - \left[1 - \frac{d + R_{\text{cross}}}{\sqrt{d^2 + R^2_{\text{cross}}}}\right] e^{-\left(R + \sqrt{d^2 + R^2_{\text{cross}}}\right)t}\Bigg).\end{aligned} \tag{3}$$

In the selective case

$$\begin{aligned}\langle I_{Az}\rangle = I^{\text{eq}}_{Az}\Bigg(1 - \left[1 + \frac{d}{\sqrt{d^2 + R^2_{\text{cross}}}}\right] e^{-\left(R - \sqrt{d^2 + R^2_{\text{cross}}}\right)t}\\ - \left[1 - \frac{d}{\sqrt{d^2 + R^2_{\text{cross}}}}\right] e^{-\left(R + \sqrt{d^2 + R^2_{\text{cross}}}\right)t}\Bigg).\end{aligned} \tag{4}$$

If $R = R^A_{\text{auto}} = R^B_{\text{auto}}$, $d = 0$ and Eqs. (3) and (4) can be simplified. In the non-selective case, only the slow component remains $(R - |R_{\text{cross}}|)$.

$$\langle I_{Az}\rangle = I^{\text{eq}}_{Az}\left(1 - 2e^{-(R - |R_{\text{cross}}|)t}\right). \tag{5}$$

In the selective case, the fast component is reintroduced

$$\langle I_{Az}\rangle = I^{\text{eq}}_{Az}\left(1 - e^{-(R - |R_{\text{cross}}|)t} - e^{-(R + |R_{\text{cross}}|)t}\right). \tag{6}$$

In a larger system, one can assume that $R = R^A_{\text{auto}} = R^B_{\text{auto}}$, $d = 0$, and spin diffusion leads to equal proton polarization i.e., $\langle I_{Az}\rangle - I^{\text{eq}}_{Az} = \langle I_{Bz}\rangle - I^{\text{eq}}_{Bz}$ hence both terms relax with a rate equal to $R - R_{\text{cross}}$. The relaxation in the selective case becomes faster and bi-exponential, which is what we observed in our experiments.

References

[1] K. Pervushin, B. Vögeli, A. Eletsky, Longitudinal ^{1}H relaxation optimization in TROSY NMR spectroscopy, J. Am. Chem. Soc. 124 (2002) 12898–12902.

[2] P. Schanda, B. Brutscher, Very fast two-dimensional NMR spectroscopy for real-time investigation of dynamic events in proteins on the time scale of seconds, J. Am. Chem. Soc. 127 (2005) 8014–8015.

[3] H.S. Attreya, T. Szyperski, G-matrix Fourier transform NMR spectroscopy for complete protein resonance assignment, Proc. Natl. Acad. Sci. USA 101 (2004) 9642–9647.

[4] K. Pervushin, R. Riek, G. Wider, K. Wüthrich, Attenuated T_2 relaxation by mutual cancellation of dipole–dipole coupling and chemical shift anisotropy indicates an avenue to NMR structures of very large biological macromolecules in solution, Proc. Natl. Acad. Sci. USA 94 (1997) 12366–12371.

[5] I.D. Campbell, R. Freeman, Influence of cross-relaxation on NMR spin-lattice relaxation times, J. Magn. Reson. 11 (1973) 143–162.

[6] A. Abragam, The Principles of Nuclear Magnetism, Clarendon Press, Oxford, 1961.

[7] M.J. Williams, I. Phan, T.S. Harvey, A. Rostagno, L.I. Gold, I.D. Campbell, Solution structure of a pair of fibronectin type 1 modules with fibrin binding activity, J. Mol. Biol. 235 (1994) 1302–1311.

[8] H. Geen, R. Freeman, Band-selective radiofrequency pulses, J. Magn. Reson. 93 (1991) 93–141.

[9] R. Koradi, M. Billeter, K. Wüthrich, MOLMOL: a program for display and analysis of macromolecular structures, J. Mol. Graph. 14 (1996) 51–55.

[10] T.S. Ulmer, I.D. Campbell, J. Boyd, Amide proton relaxation measurements employing a highly deuterated protein, J. Magn. Reson. 166 (2004) 190–201.

[11] L. Kay, P. Keifer, T. Saarinen, Pure absorption gradient enhanced heteronuclear single quantum correlation spectroscopy with improved sensitivity, J. Am. Chem. Soc. 114 (1992) 10663–10665.

[12] T.J. Norwood, J. Boyd, J.E. Heritage, N. Soffe, I.D. Campbell, J. Magn. Reson. 87 (1990) 488–501.

[13] E. Kupče, J. Boyd, I.D. Campbell, Short selective pulses for biochemical applications, J. Magn. Reson. B 106 (1995) 300–303.

[14] A.B. Sibley, M. Cosman, V.V. Krishnan, An empirical correlation between secondary structure content and averaged chemical shifts in proteins, Biophys. J. 84 (2003) 1223–1227.

[15] T. Wu, K.R. Kendell, J.P. Felmlee, B.D. Lewis, R.L. Ehman, Reliability of water proton chemical shift temperature calibration for focused ultrasound ablation therapy, Med. Phys. 27 (2000) 221–224.

[16] N.J. Baxter, M.P. Williamson, Temperature dependence of ^{1}H chemical shifts in proteins, J. Biomol. NMR 9 (1997) 359–369.